12th INTERNATIONAL SCIENTIFIC CONFERENCE ON DEFENSIVE TECHNOLOGIES
OTEH 2026
Serbia, Tara, 21 - 24 October 2026

REACH AND WORKSPACE ENVELOPE ANALYSIS OF THE SIX-DOF ARTICULATED ROBOT ARMA6

JELENA VIDAKOVIĆ
Lola Institute, Belgrade, jelena.vidakovic@li.rs

ANDRIJA DEVIĆ
Lola Institute, Belgrade, andrija.devic@li.rs

GORAN VASILIĆ
Lola Institute, Belgrade, goran.vasilic@li.rs

NIKOLA ŽIVKOVIĆ
Lola Institute, Belgrade, nikola.zivkovic@li.rs

IVANA VASOVIĆ MAKSIMOVIĆ
Lola Institute, Belgrade, ivana.vasovic@li.rs

Abstract: *This paper presents the reach and position workspace envelope analysis of the six-degree-of-freedom articulated robot ARma6 based on the solution of its forward kinematic problem. The robot reach is determined by combining Monte Carlo sampling with nonlinear optimization, while the limits of Tool Centre Point (TCP) in Cartesian space are obtained analytically using trigonometric relations. The rotational symmetry of the positional workspace is exploited to simplify the three-dimensional positional workspace's envelope determination, with two approaches considered: numerical extraction of the inner and outer radial boundaries and a geometric approach based on the circular TCP path corresponding to the effective robot reach. The obtained results characterize the reach and position workspace of the ARma6 robot and provide a basis for further evaluation of its geometry during the design process.*

Keywords: *robot, kinematics, reach, workspace, forward.*

1. INTRODUCTION

Growing customer demands and global competition are amongst the key drivers of the increasing need for integrating industrial robots with Industry 4.0 solutions [1]. Flexible robotic systems can adapt to a variety of tasks and products, making them particularly advantageous for high-mix, low-volume manufacturing, which is typical for small and medium-sized enterprises (SMEs) [1-2]. However, the wider adoption of industrial robots in SMEs remains limited by factors such as investment costs and the expertise required for robot programming [1-4]. These challenges encourage the development of more accessible robotic solutions for SMEs. In this context, the ARma6 robotic system, Fig.1, is being developed as a compact six degrees of freedom (DoFs) articulated robot supported by an extended reality (XR)-based platform for robot programming and interaction [5].

Solution of the robot forward kinematics problem (FK algorithm) is used to determine the position and orientation of the robot end-effector, i.e. frame attached to its TOOL CENTRE POINT (TCP) with respect to (w.r.t.) the BASE frame, for the input joint variables [6-7]. FK serves as the basis for robot simulation, inverse kinematics (IK) and motion planning, and workspace analysis.

Robot workspace and reach are amongst the key considerations in robot design, as they provide a quantitative measure of the range of tasks that the robot can perform. Additionally, before applying the IK algorithm, it is useful to verify whether the desired TCP position lies within the robot reach, position limits, or within its workspace, allowing the user to distinguish potential workspace-related errors from other IK failures. The workspace is often broken down into a reachable (position) workspace - the entire set of points reachable by the manipulator, and a dexterous workspace - points that the manipulator can reach with an arbitrary orientation of the end-effector [8-9].

In this paper, the FK algorithm, robot reach calculation, and position workspace envelope determination of the ARma6 articulated robot are presented. The robot reach is determined numerically using nonlinear optimization. Additionally, the limits of the TCP position in Cartesian space are obtained analytically using trigonometric identities. The methodology for the positional workspace envelope determination is presented.

This paper is divided as follows. In Section 2, the FK algorithm for the ARma6 robot is presented. The methodology for determining a robot reach and position

Corresponding author: J. Vidakovic;
E-mail: jelena.vidakovic@li.rs
DOI: 10.5937/OTEH26072V

workspace envelope is presented in Section 3, and numerical simulation results are also presented herein. Discussion is given in Section 4, while concluding remarks are given in Conclusion.



Figure 1. 3D model of the ARma6 robot

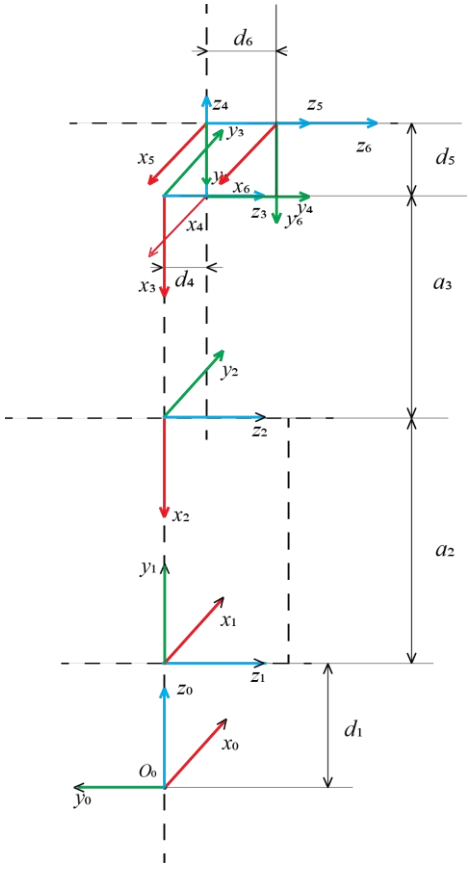


Figure 2. Frames assigned to ARma6 joints [5]

2. FORWARD KINEMATICS ALGORITHM

One of the most used methods for kinematic modeling in robotics, the Denavit-Hartenberg (DH) convention [10], is adopted in this study. Robot DH parameters, Table 1, are defined based on frames attached to robot joints, Fig. 2 [5].

Table 1. Denavit-Hartenberg parameters for ARma6

Joint i	a_i	α_i	d_i	a_i
1	0	90°	d_1	θ_1
2	a_2	0	0	$\theta_2 - 90$
3	a_2	0	0	θ_3
4	0	90°	d_4	$\theta_4 - 90$
5	0	-90°	d_5	θ_5
6	0	0	d_6	θ_6

Joint-to-joint homogeneous transformation matrix (HTM) describing coordinate frame i relative to frame i-1 using DH parameters is given as follows [11]:

$$\mathbf{A}_i = \mathrm{Rot}(z_{i-1},\theta_i)\mathrm{Trans}(z_{i-1},d_i)\mathrm{Trans}(x'_{i-1},a_i)\mathrm{Rot}(x'_{i-1},\alpha_i) \quad (1)$$

Based on joint-to-joint HTMs, the HTM of the frame attached to the robot's TCP w.r.t. the BASE frame is obtained as:

$$\mathbf{T}_{06}(\mathbf{q}) = \mathbf{A}_1\mathbf{A}_2\mathbf{A}_3\mathbf{A}_4\mathbf{A}_5\mathbf{A}_6 \quad (2)$$

In Eq. (2), $\mathbf{q} = [q_1 \ \ldots \ q_n]$ is a vector defining the robot configuration (joint positions q_i for i-1..n, where n is the number of DoFs, i.e. 6 for ARma6).

Hereinafter, the following notation is adopted:
$c_i = \cos(q_i)$, $s_i = \sin(q_i)$,
$c_{ij} = \cos(q_i + q_j)$, $s_{ij} = \sin(q_i + q_j)$,
$c_{ijk} = \cos(q_i + q_j + q_k)$, $s_{ijk} = \sin(q_i + q_j + q_k)$

When the HMT $\mathbf{T}_{06}(\mathbf{q})$ is defined, the pose of the TCP w.r.t. the BASE frame can be calculated for every time instance t, i.e. the robot configuration $\mathbf{q}(t)$ given that $\mathbf{T}_{06}$ contains the rotation matrix and the position vector of the TCP frame and its origin w.r.t. the BASE frame [6]. X, Y, Z coordinates are obtained from the fourth column of the matrix $\mathbf{T}_{06}$ given in Eq. (2) as follows:

$$X(\mathbf{q}) = d_6(c_5s_1 + c_{234}c_1s_5) + d_4s_1 - a_2c_1s_2 - d_5s_{234}c_1 - a_3c_1c_2s_3 - a_3c_1s_2c_3 \quad (3)$$

$$Y(\mathbf{q}) = d_6(c_{234}s_1s_5 - c_1c_5) - a_2s_1s_2 - d_5s_{234}s_1 - a_3s_1s_{23} - d_4c_1 \quad (4)$$

$$Z(\mathbf{q}) = d_1 + a_3 c_{23} + a_2 c_2 + d_5 c_{234} + d_6 s_5 s_{234} \quad (5)$$

TCP frame orientation is obtained using the RPY angles convention [12] as given in [5].

3. DETERMINATION OF ROBOT REACH AND POSITION WORKSPACE ENVELOPE

Both the robot reach and the size of the workspace envelope are fundamental geometric characteristics that strongly influence the mechanical design and application of robotic manipulators. Increasing the workspace and reach typically requires longer links, which generally reduce manipulator stiffness and positioning accuracy. For the ARma6 robot and its adopted payload, a target reach of approximately 1 m was selected during the initial design stage, resulting in a compact robot configuration with a workspace suitable for the intended development and experimental activities.

3.1. Robot reach determination

In industrial robot specifications, the reach is commonly reported as the maximum distance from the robot BASE FRAME origin to the TCP, here denoted as $R_{\max}$, or as the maximum horizontal radial distance of the TCP to the BASE FRAME vertical axis, here denoted as $\rho_{\max}$.

$$R_{\max} = \max \sqrt{X^2 + Y^2 + Z^2} \quad (6)$$

$$\rho_{\max} = \max \sqrt{X^2 + Y^2} \quad (7)$$

Taking into account Eqs. (3) and (4), and by using simple trigonometric identities, the distance $\rho(\mathbf{q})$ from Eq. (7), i.e. the horizontal radial reach, can be calculated as

$$\rho(\mathbf{q}) = \sqrt{A^2 + B^2} \quad (8)$$

where

$$A = A(\mathbf{q}) = d_6 c_{234} s_5 - a_2 s_2 - d_5 s_{234} - a_3 s_{23} \quad (9)$$

$$B = B(\mathbf{q}) = d_4 + d_5 c_5 \quad (10)$$

The robot reach $R_{\max}$ can be calculated using several different approaches. Although the reach may be estimated by evaluating the FK over a discretized joint space, such an approach does not guarantee that the global maximum is found. Calculating reach for selected DH parameters can be regarded as a nonlinear optimization problem in which the joint variables q_1,.., q_6 are treated as optimization variables and the Euclidean distance from the robot BASE FRAME origin to the TCP is maximized. Given that the reach function is a highly nonlinear trigonometric function of multiple joint variables, obtaining a closed-form solution is generally challenging. In this study, numerical approaches are utilized.

It can be seen from Eq. (5-6) and Eqs. (8-10) that $Z(\mathbf{q})$ and $\rho(\mathbf{q})$ and consequently $R(\mathbf{q})$ do not depend on q_1 and q_6. Consequently, herein the maximum reach was determined numerically for the selected DH parameters by „optimizing“ the joint variables q_2, to q_5. The following two-stage procedure was applied for $R_{\max}(\mathbf{q})$ calculation:

1. Generate a large number of random initial configurations within the admissible joint space using Monte Carlo [13] sampling.
2. Starting from each initial configuration, locally optimize the objective function. The largest value obtained from all optimization runs is taken as the estimated global maximum reach.

On another note, since d_1 represents a fixed offset between the BASE FRAME and the second joint, it is convenient to define the effective robot reach $R_{1\max}$ w.r.t. the frame attached to the second joint, as illustrated in Fig. 3. The effective robot reach is calculated as:

$$R_{1\max} = Z_{\max} - d_1 \quad (11)$$

For calculation of $Z_{\max}$, the approach using trigonometric identities (without optimization methods) is applied herein. From Eq. (5), it can be seen that for the maximum TCP's Z coordinate w.r.t. the BASE FRAME, the robot configuration has to be the following: $q_2 = 0$, $q_2 + q_3 = 0 \rightarrow q_3 = 0$, $q_5 = \pi/2$. For the adopted values, the expression:

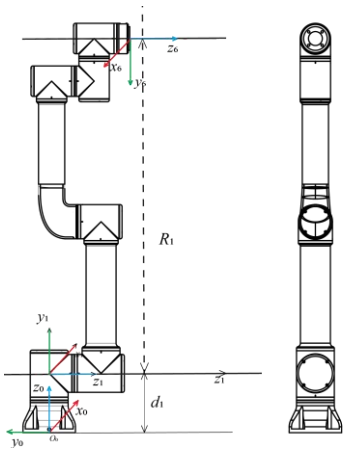


Figure 3. Robot ARma6 model selected frames.

$$d_5 c_{234} + d_6 s_{234} \quad (12)$$

has the maximum $\sqrt{d_5^2 + d_6^2}$ for the value of q_4:

$$q_4 = \alpha, \ \alpha = a\tan 2(d_6, d_5) \quad (13)$$

and the following is obtained:

$$Z_{\max} = d_1 + a_2 + a_3 + \sqrt{d_5^2 + d_6^2} \quad (14)$$

$$Z_{\min} = d_1 - a_2 - a_3 - \sqrt{d_5^2 + d_6^2} \quad (15)$$

3.2. Robot position workspace envelope determination

The workspace envelope encloses the workspace. Based on the FK algorithm, Eqs. (3-5), the position workspace can be calculated numerically. From Eq. (5) and Eqs. (8-10), it can be seen that neither the radial distance $\rho(Z)$ of the TCP from the BASE FRAME vertical axis, i.e., z_0 axis from Fig.2, nor the TCP's Z coordinate depend on the angle q_1. The joint angle q_1 changes only the azimuthal position of the TCP about the z_0 axis. From this, it can be concluded that the positional workspace of the ARma6 robot is rotationally symmetric around the BASE FRAME vertical axis.

In this study, the positional workspace envelope was determined using two approaches. In both approaches, the analysis was performed for an adopted constant value of q_1, and the obtained two-dimensional geometric representation was subsequently revolved about the z_0 axis, Fig. 2, to generate the three-dimensional workspace envelope. Approach 1 is based on the numerical determination of the inner and outer workspace boundaries in the ρ-Z plane. Approach 2 is based on the determination of the complete circular TCP path obtained by the rotation of the robot arm corresponding to the effective robot reach $R_{1\max}$, Eq. (11), Fig. 3, about the z_1 axis, $q_2 \in [0,\ 2\pi]$.

Approach 1

In Approach 1, the three-dimensional positional workspace is determined by one meridional cross-section (e.g. $q_1 = 0$). The Cartesian coordinates are transformed into cylindrical coordinates (ρ, Z). The inner $\rho_{\min}(Z)$ and outer $\rho_{\max}(Z)$ boundaries of the meridional section are determined using the following numerical procedure:

1. Perform a grid search [14] over the selected joint variables. Compute the TCP coordinates (X, Y, Z) using the FK for all sampled joint configurations and calculate the corresponding radial distance ρ, Eqs. (8-10).
2. Divide the range of Z-coordinates into a predefined number of horizontal layers of equal thickness. For each layer, identify all sampled points whose Z-coordinates lie within the corresponding interval.
3. Determine the inner and outer boundaries of all layers as the minimum and maximum values of $\rho(Z)$ among the selected points.
4. After obtaining the inner $\rho_{\min}(Z)$ and outer $\rho_{\max}(Z)$ boundaries for each layer in $Z \in [Z_{\min}, Z_{\max}]$ as an array of discrete values, connect them by linear interpolation.
5. Revolve interpolated $\rho_{\min}(Z)$ and $\rho_{\max}(Z)$ curves about the the base-frame vertical z_0 axis.

Approach 2

The second approach in generating the outer workspace envelope is based on the complete rotation of the robot arm about the z_1 axis, $q_2 \in [0,\ 2\pi]$ in the configuration corresponding to the effective robot reach $R_1 = R_{1\max}$, for for an arbitrary adopted value of q_1 angle (herein it is adopted that $q_1 = 0$). The circular TCP path can be obtained either analytically, using the parametric equation of a circle with the previously determined center and radius $r = R_{1\max}$, or numerically, using the FK for a complete variation of the corresponding joint angle $q_2 \in [0,\ 2\pi]$. In both cases, the obtained TCP coordinates are subsequently transformed by the rotation matrix about the BASE FRAME vertical axis. The procedure consists of the following steps:

1. Determine the effective robot reach $R_{1\max}$, the corresponding robot configuration $q_{2\ldots}q_5$, and the center C_0 of the resulting TCP circle.
2. Generate the circular TCP path either from its parametric equation or directly from the FK by varying the corresponding joint angle through a complete revolution.
3. Revolve the obtained circular TCP path about the BASE FRAME vertical axis by applying the corresponding rotation matrix to the TCP position vectors $[\mathbf{X}\ \mathbf{Y}\ \mathbf{Z}]^T$.

3.3. Numerical results

For numerical calculation, the following DH parameters have been adopted: d_1=158.09mm, d_4=101mm, d_5=86mm, d_6=90.29mm, a_2=158.09mm, a_3=158.09mm.

For the selected DH parameters, 50000 random initial configurations of the joint variables q_2, q_3, q_4, q_5 were generated using Monte Carlo sampling within the range [0, 2π]. Starting from each initial configuration, a constrained local optimization was performed in Matlab [15]. The maximum reach obtained was $R_{\max} = 110.54$cm for $q_2 \approx$ -0.03°, $q_3 \approx$ 0.02°, q_4= -46.11°, q_5=-81.83°.

From Eq. (14-15), based on adopted DH parameters, it is obtaoned that $Z_{\max}$ =110.02 cm, $Z_{\min}$ =-78.4 cm. From Eq. (13) and Eq. (11), it is obtained that α=46.39°, and $R_{1\max} = 94.21$ cm.

The radial boundary values $\rho_{\min}(Z)$ and $\rho_{\max}(Z)$ were determined numerically using a uniform grid search over q_2, q_3, q_4, q_5 within [−π,π], with a discretization step of 5°, the resulting range of Z-coordinates was divided into 150 horizontal layers, and the following is obtained: $\rho_{\max} = 94.83$ cm.

Herein, since the q_6 angle does not affect the position of the TCP, it is adopted that $q_6 = 0$. For the adopted numerical values of DH parameters, the inner and outer boundaries of the meridional cross-section are depicted in Fig. 4.

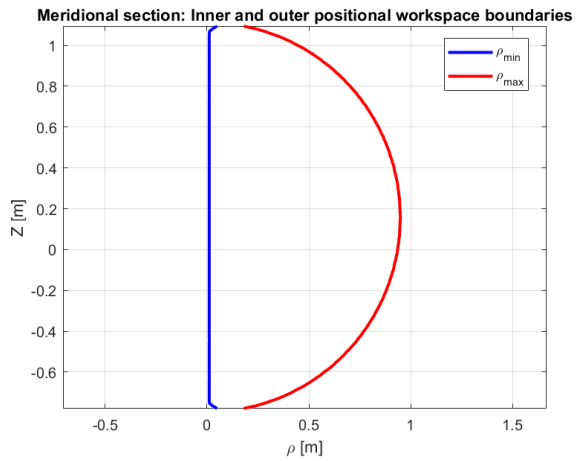


Figure 4 The inner and outer boundaries of the meridional cross-section.

The workspace envelope obtained using Approach 1 is shown in Fig. 5. By rotating $\rho_{\min}(Z)$ and $\rho_{\max}(Z)$ around the z_0 axis, the positional workspace envelope for the ARma6 robot is obtained from 120 angular samples.

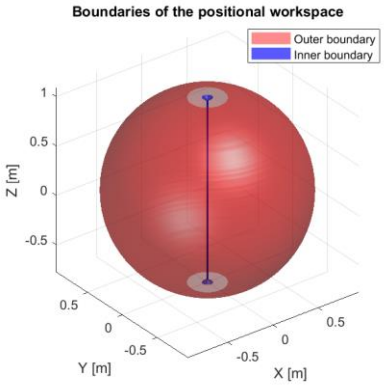


Figure 5 Positional workspace envelope for Arma6 robot obtained by applying Approach 1

To compare the two approaches, Fig. 6 superimposes 25 circular TCP paths corresponding to the effective reach $R_{1\max}$, onto the numerically determined workspace envelope by Approach 1. The circular paths closely follow the outer boundary obtained using Approach 1, indicating good agreement between the two approaches.

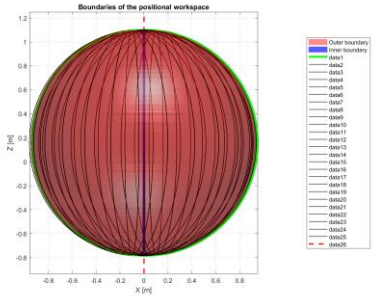


Figure 6 Positional workspace envelope for ARma6 robot obtained by applying Approach 1 and Approach 2 at 25 positions of the $R_{1\max}$ circle around the BASE FRAME vertical axis.

4. DISCUSSION

The proposed methodology combines analytical and numerical approaches for evaluating the kinematic characteristics of articulated manipulators. While the forward kinematic model provides analytical expressions for the TCP position, numerical optimization enables an accurate determination of the maximum reach without relying on exhaustive discretization of the joint space. Furthermore, exploiting the rotational symmetry of the manipulator positional workspace allows the analysis to be performed for a single value of the first joint angle, significantly reducing the computational effort required for three-dimensional workspace determination.

The obtained reach and position workspace envelope provide useful geometric information during the conceptual design stage, i.e. quantitative measures and quick assessment of the robot operating range and the comparison of different manipulator geometries. Since both characteristics depend directly on the selected DH parameters, the proposed methodology can support the selection of appropriate link dimensions in the early stages of robot design before detailed structural and dynamic analyses are performed. When designing a robot, an increase in reach is obtained by increasing the length of the robot's links, however this causes an increase in the mass of the links, the required motor torques, a decrease in stiffness and potentially the accuracy, and the robot may be more prone to vibrations.

In future work, the obtained reach and position workspace envelope can be incorporated into multi-objective optimization procedures aimed at identifying the optimal geometric parameters of the robot. Such optimization could simultaneously consider workspace characteristics, reach, structural stiffness, payload capacity, joint torques, and manipulator mass, resulting in improved overall robot performance. Additionally, the presented methodology should be extended by incorporating self-collision constraints.

5. CONCLUSION

This paper presented the determination of the reach and the position workspace envelope for the six DoF articulated robot ARma6 using its analytical FK model. The reach was obtained numerically using Monte Carlo sampling and nonlinear optimization, and the limits of Cartesian coordinates were determined analytically using trigonometric identities. Two approaches were applied to the position workspace envelope determination. In both approaches, the analysis was performed for a constant value of the first joint angle, and the resulting two-dimensional geometry was subsequently revolved about the base frame vertical axis in order to obtain the three-dimensional workspace envelope. In Approach 1, the rotational symmetry of the manipulator positional workspace was exploited to reconstruct the workspace envelope from the numerically determined inner and outer boundaries of a single meridional cross-section. In Approach 2, the outer workspace envelope was determined geometrically from the circular TCP path

corresponding to the effective robot reach. The obtained numerical results characterize the reach and position workspace of the current ARma6 geometry and provide a basis for further evaluation of the manipulator geometry during the design process. Future work will extend the workspace analysis by incorporating self-collision constraints and investigating the influence of the robot geometric parameters on the usable workspace using a multi-objective optimization framework. Additionally, the obtained workspace envelope will be integrated and visualized within the ARma6 XR environment to support intuitive robot task planning.

Acknowledgment

This research has been supported by the research grants of the Serbian Ministry of Science, Technological Development, and Innovations, Grant No. 451-03-33/2026-03/ 200066

References

[1] ONG, S.K., YEW, A.W.W., THANIGAIVEL, N.K., NEE, A.Y.C.: Augmented Reality-Assisted Robot Programming System for Industrial Applications, Robot. Comput.-Integr. Manuf., 61 (2020) 101820.

[2] DEVIC, A., VIDAKOVIC, J., ZIVKOVIC, N.: Development of Standalone Extended-Reality-Supported Interactive Industrial Robot Programming System, Machines, 12(7) (2024) 480.

[3] RIVERA-PINTO, A., KILDAL, J.: From Digital Twin Towards Shop Floor: Codeless Programming of Pick-and-Place Robots Through Extended-Reality Interaction, Proceedings of the Conference on Production Systems and Logistics: CPSL 2026, Offenburg, 2026, pp. 391–400.

[4] BROGÅRDH, T.: Present and Future Robot Control Development—An Industrial Perspective, Annu. Rev. Control, 31 (2007) 69–79.

[5] VIDAKOVIC, J., DEVIC, A., DIMIC, Z., ZIVKOVIC, N., LAZAREVIC, I.: A Solution to the Forward Kinematic Problem of the ARma6 Robot, Proceedings of the 25th International Symposium INFOTEH-JAHORINA, 2026.

[6] ASPRAGATHOS, N.A., DIMITROS, J.K.: A Comparative Study of Three Methods for Robot Kinematics, IEEE Trans. Syst., Man, Cybern. B, 28(2) (1998) 135–145.

[7] LYNCH, K.M., PARK, F.C.: Modern Robotics: Mechanics, Planning, and Control, Cambridge University Press, Cambridge, 2017.

[8] SPONG, M.W., VIDYASAGAR, M.: Robot Dynamics and Control, John Wiley & Sons, New York, 2008.

[9] ORLANDO, E.M., NENNA, F., LORUSSO, F.M., MINGARDI, M., BUODO, G., GAMBERINI, L.: Capturing Shared Actions and Coordination in Collaborative Workspaces: A Markerless Pipeline for Synchronized Human–Robot 3D Pose Estimation, IEEE Access, 14 (2026) 67101–67114.

[10] DENAVIT, J., HARTENBERG, R.S.: A Kinematic Notation for Lower-Pair Mechanisms Based on Matrices, J. Appl. Mech., 22 (1955) 215–221.

[11] SICILIANO, B., SCIAVICCO, L., VILLANI, L., ORIOLO, G.: Robotics: Modelling, Planning and Control, Springer, London, 2009.

[12] KVRGIC, V.: Development of Intelligent System for Control and Programming of Industrial Robots, Doctoral Dissertation, Faculty of Mechanical Engineering, University of Belgrade, Belgrade, 1998.

[13] METROPOLIS, N., ULAM, S.: The Monte Carlo Method, Journal of the American Statistical Association, 44(247) (1949) 335–341.

[14] LAVALLE, S.M., BRANICKY, M.S., LINDEMANN, S.R.: On the Relationship Between Classical Grid Search and Probabilistic Roadmaps, International Journal of Robotics Research, 23(7–8) (2004) 673–692.

[15] THE MATHWORKS, INC.: MATLAB, The MathWorks, Inc., Natick, Massachusetts, US